Chronic Hypoperfusion is not Associated with Cerebral Amyloidosis

Dong-Yu Fan
Third Military Medical University Daping Hospital and Research Institute of Surgery
Hui-Yun Li
Third Military Medical University Daping Hospital and Research Institute of Surgery
Dong-Wan Chen
Third Military Medical University Daping Hospital and Research Institute of Surgery
Yang Chen
Third Military Medical University Daping Hospital and Research Institute of Surgery
Xu Yi
Third Military Medical University Daping Hospital and Research Institute of Surgery
Heng Yang
Third Military Medical University Daping Hospital and Research Institute of Surgery
Qian-Qian Shi
Third Military Medical University Daping Hospital and Research Institute of Surgery
Fang-Yang Jiao
Third Military Medical University Daping Hospital and Research Institute of Surgery
Yi Tang
Third Military Medical University Daping Hospital and Research Institute of Surgery
Qi-Ming Li
Third Military Medical University Daping Hospital and Research Institute of Surgery
Fang-Yang Wang
Third Military Medical University Daping Hospital and Research Institute of Surgery
Shu-Nan Wang
Third Military Medical University Daping Hospital and Research Institute of Surgery
Rong-Bing Jin
Third Military Medical University Daping Hospital and Research Institute of Surgery
Fan Zeng
Third Military Medical University Daping Hospital and Research Institute of Surgery
Yan-Jiang Wang (yanjiang_wang@tmmu.edu.cn)
Department of Neurology and Center for Clinical Neuroscience, Daping Hospital,Third Minitary Medical University, Chongqing 400042, China https://orcid.org/0000-0002-6227-6112

Short report

Keywords: cerebral hypoperfusion, β-amyloid, brain atrophy, Alzheimer's disease

Posted Date: November 13th, 2020

DOI: https://doi.org/10.21203/rs.3.rs-104777/v1

Chronic hypoperfusion is not associated with cerebral amyloidosis

Running head: hypoperfusion and amyloidosis

Dong-Yu Fan[1,2,3], Hui-Yun Li[1,2,3], Dong-Wan Chen[1,2,3], Yang Chen[1,2,3], Xu Yi[1,2,3], Heng Yang[1,2,3], Qian-Qian Shi[1,2,3], Fang-Yang Jiao[4], Yi Tang[4], Qi-Ming Li[4], Fang-Yang Wang[4], Shu-Nan Wang[5], Rong-Bing Jin[4], Fan Zeng[1,2,3,*], Yan-Jiang Wang[1,2,3,*]

1. Department of Neurology and Centre for Clinical Neuroscience, Daping Hospital, Third Military Medical University, Chongqing, China.
2. Institute of Brain and Intelligence, Third Military Medical University, Chongqing, China.
3. Chongqing Key Laboratory of Ageing and Brain Diseases, Chongqing, China.
4. Department of Nuclear Medicine, Daping Hospital, Third Military Medical University, Chongqing, China.
5. Department of Radiology, Daping Hospital, Third Military Medical University, Chongqing, China.

* Correspondence to yanjiang_wang@tmmu.edu.cn (Y.J.W.) or zengfan326@163.com (F.Z.)

Tables: 1; Figures: 3

Word Count: 2215

Abstract

Background

Insufficient cerebral perfusion is suggested to play a role in the development of AD. We investigated the effect of chronic cerebral hypoperfusion on AD-related pathology, including β-amyloid (Aβ) deposition and brain atrophy in humans.

Methods

We enrolled 10 cognitively normal patients (median age: 64 years old) with unilateral chronic cerebral hypoperfusion. Volumes of interest (VOIs) and regions of interest (ROIs) with the most pronounced hypoperfusion changes were created in the hypoperfused region, and were then mirrored into the contralateral hemisphere to create a control region with normal perfusion respectively.11C-Pittsburgh compound-PET (PiB-PET) imaging standard uptake ratios (SUVRs) and several brain atrophy indices from the CT images of each patient were calculated.

Results

We found that there were no differences in SUVRs of PiB-PET imaging and brain atrophy indices between the hypoperfused regions and contralateral normally-perfused regions.

Conclusion

Our findings suggest that chronic hypoperfusion may not directly induce cerebral Aβ deposition and neurodegeneration in humans.

Keywords: cerebral hypoperfusion; β-amyloid; brain atrophy; Alzheimer's disease

Abbreviations:

β-amyloid (Aβ)

Volume of interest (VOI)

region of interest (ROI)

^{11}C-Pittsburgh compound-PET (PiB-PET)

standard uptake ratios (SUVRs)

Introduction

Alzheimer's disease (AD) is the most common form of aging-related dementia, placing a heavy burden on patients and society (1, 2). β-amyloid (Aβ) deposition is considered to be the key event of AD pathogenesis. However, the causes of AD remain unclear (3).

There is a significant decrease in cerebral blood flow and insufficient perfusion in the brain of AD patients (4). And the lack of perfusion has already occurred in the brains of mild cognitive impairment (MCI) patients (5, 6), which is related to the rate of cognition decline. A recent study on the ADNI database discovered that in the progression from a healthy state to AD, insufficient cerebral perfusion may play an important role in initiating AD (7). In addition, vascular risk factors, such as hypertension, diabetes mellitus, heart diseases and hypercholesterolemia, are associated with the increased risk of AD, exacerbation of cognitive decline and neurodegeneration, and amyloid deposition, which is presumed to be caused by chronic cerebral hypoperfusion (8-10), supporting the causative roles of chronic cerebral hypoperfusion in the development of AD.

However, despite chronic cerebral hypoperfusion modeled with bilateral or unilateral common carotid arteries surgical ligation increased Aβ deposition and neurodegeneration in AD animals (11, 12), no correlation between local amyloid deposition and local cerebral hypoperfusion was observed in humans (13-15). In this study, we investigated the impact of chronic cerebral hypoperfusion on amyloid

74 deposition and neurodegenerative changes in a group of cognitively normal patients
75 with chronic unilateral cerebral hypoperfusion.
76
77 # Methods
78 ## Study subjects
79 Patients with chronic unilateral cerebral hypoperfusion were recruited from the
80 Registry of Neurodegeneration of Daping Hospital from January 2016 to December
81 2019. Chronic unilateral cerebral hypoperfusion was defined as the reduced perfusion
82 of one cerebral hemisphere in CT perfusion (CTP) with or without severe middle
83 cerebral artery (MCA) / internal carotid artery (ICA) stenosis; the contralateral
84 cerebral hemisphere of the same patient was set as the control. The subjects were not
85 eligible if they had (1) cognition decline caused by neurological diseases (e.g., AD,
86 MCI, vascular dementia, Parkinson's disease dementia, etc.); (2) a history of stroke,
87 intracranial infection or brain trauma; (3) heart diseases (severe coronary heart disease,
88 cardiac insufficiency, atrial fibrillation, etc.); (4) severe liver renal and pulmonary
89 insufficiency; (5) concomitant disorders including hematological diseases, peptic
90 ulcer, mental illness and epilepsy; (6) an allergy to ^{11}C-Pittsburgh compound.
91 ## Clinical assessments
92 Demographic characteristics including age, sex, and education levels were recorded.
93 All subjects underwent clinical assessments including medical history, physical
94 examination, laboratory tests, APOE genotyping, and neuropsychological tests. CT,
95 CT angiography (CTA), CT perfusion (CTP), and ^{11}C-Pittsburgh compound-positron

emission tomography (PiB-PET) examinations were performed. Mini-Mental State Examination (MMSE) and Clinical Dementia Rating (CDR) were administered to screen and assess the overall cognitive function (16).

Neuroimaging

NECT / CTP / CTA acquisition. NECT / CTP / CTA were sequentially performed on a 256-slice multidetector CT scanner (Brilliance iCT, Philips Healthcare). The parameters were as following. NECT : slice thickness = 5 mm , interlayer spacing =5mm, 120KV, 150mAs. CTP: 16 cm coverage in the z-axis, 80 kV, 100 mA. Total acquisition time was 60 seconds (30 consecutive spiral acquisitions of 2 seconds each). A total of 50 mL of contrast agent (Iopromide, Ultravist-370, Bayer Schering Pharma) was injected intravenously followed by a 50-mL saline flush at 6.5 mL/s. CTA : coverage from vertex to aortic arch, slice thickness = 0.625 mm , interlayer spacing =0.625mm, 100KV, 150mAs, A total of 50 mL of contrast agent (Iopromide, Ultravist-370, Bayer Schering Pharma) was injected intravenously followed by a 50-mL saline flush at 5.0 mL/s.

CTP data were processed using postprocessing station (IntelliSpace Portal, Philips). First, the arterial input function was detected manually using a ROI on anterior cerebral artery to generate the perfusion parametric maps, including CBF, CBV, MTT and TTP.

PET acquisition. All subjects were required to fast for at least 6 hours but had free access to water before the PET scan. PET scans were performed with a Siemens Biograph 64 PET/CT machine (Siemens, Munich, Germany) in the three-dimensional

model. PiB-PET was performed according to standardized research protocols (17). A dynamic 90 minutes emission scan was administered with an intravenous injection of ^{11}C-PiB after 10 minutes of transmission scan. Standardized images were extracted within the regulated interval time after injection. All scans were performed in a dimly lit and quiet room with subjects in a resting state.

Image analysis

β-amyloid burden. CapAIBL (Australian eHealth Research Centre, CSIRO, Australian) was used to calculate the cortical SUVRs (18) and determine the negative or positive of PiB-PET amyloid burden using the cut-off value of 1.42 (19). Pmod software (version 3.5, Pmod technologies, Zurich, Switzerland) was used to analyze the amyloid burden in the volume of interest (VOI) and region of interest (ROI). PiB-PET series and standard MRI-T1 templates were spatially merged by the fusion module. VOI and ROI were created in the MRI images according to the MTT and CBF of CTP by a researcher blinded to the PET images. A sphere (VOI) with a diameter of 15 mm was created in the region with the most pronounced hypoperfusion changes of each subject, and an irregular ROI was manually drawn to cover the hypoperfused region as much as possible. The hypoperfused VOI and ROI were then mirrored into the contralateral hemisphere to create a control region with normal perfusion. For 3 cases with minor infarcts, the infarction regions were completely avoided in VOI and ROI.

All regions were then intersected using the gray/white matter segmentation mask into VOI (or ROI) and control. The SUVR of cortex and white matter in each region was

subsequently measured using the cerebellar composite gray matter as the reference region.

Brain atrophy. In all the patients, the brain atrophy indices were measured on the CT scans, based on the commonly-used method described by Meese (20). These indices, including Bicaudate index, Bifrontal index, Evans index, Cella index, Celda media index, Ventricular index, were calculated unilaterally by the distance from the midline of the brain (shown in detail in Fig. 2) (21, 22). Every index was measured twice and the mean value was calculated to increase accuracy and limit the "partial volume" effect by RadiAnt DICOM Viewer 5.0.1 (Medixant, Poznan, Poland).

Statistics analyses

The Shapiro-Wilk test was used to test for normal distribution. The differences in SUVRs and atrophy indices of bilateral cerebral hemispheres between the hypoperfused regions (Hypo) and the normally-perfused contralateral regions (Ctrl) were analyzed using Wilcoxon's-signed test. All hypothesis-testing was two-sided, and statistical significance was defined as $P < 0.05$. All statistical computations were performed using SPSS version 19.0 (SPSS, Inc., Chicago, IL).

Data availability

The data that support the findings of this study are available on request from the corresponding author. The data are not publicly available as they include information that could compromise the privacy of the research participants

Results

Characteristics of the study subjects

Subjects' characteristics were shown in Table 1. Fourteen patients met the inclusion criteria, eleven patients agreed to participate, and finally ten of them completed the study. The median age of the 10 participants, consisting of 4 males and 6 females, was 64 years (47-76 years). All participants met the criteria for extensive CTP decline in the unilateral hemisphere without clinical manifestations of acute stroke or cognition impairment. Six cases had occlusions in the ICA or MCA, while 3 cases had severe stenosis of ICA or MCA, and 1 case had the left frontal patchy hypoperfusion without obvious large vessel stenosis.

Hypoperfusion and β-amyloid burden

In all subjects, there was no significant difference in β-amyloid deposition between the hypoperfused regions (represented by VOI and ROI) and the normally perfused contralateral regions. In the spherical VOI where the hypoperfusion was most pronounced, the median cortical SUVR was not different from those in the contralateral regions (1.11 [IQR 1.02-1.11] vs. 1.10 [IQR 1.02-1.13], P=0.721) (Fig. 1A). In the ROI covering as much hypoperfused region as possible, the median cortical SUVR (1.11 [IQR 1.09-1.12]) was similar to those in the contralateral regions (1.10 [IQR 1.09-1.13]) (P=0.241) (Fig. 1B). Of note, one subject had bilateral abnormal ^{11}C-PiB uptake (composite score SUVR >1.42, Fig. 3D).

There is a possibility that the cortical SUVR in the hypoperfused regions might be underestimated due to the less delivery of radiotracer to these regions. To correct the possible tracer entry error due to hypoperfusion, we evaluated the grey matter/white

matter retention ratio (GM/WM) and found that there were no significant differences in VOI (Hypoperfused vs. Contralateral: 0.77 [IQR 0.71–0.87] vs. 0.78 [IQR 0.76–0.87], *P*=0.333) and ROI (Hypoperfused vs. Contralateral: 0.84 [IQR 0.84–0.85] vs. 0.84 [IQR 0.84–0.85], *P*=0.445) (Fig. 1C and D) between the hypoperfused and contralateral regions.

Hypoperfusion and neurodegeneration

The neurodegeneration indicated by the brain atrophy was further evaluated. In the 10 subjects, there were no significant differences in brain atrophy indices between the hypoperfused hemispheres and contralateral hemispheres, including Bicaudate index (hypoperfused vs. contralateral: 0.11 [IQR 0.10–0.13] vs. 0.13 [IQR 0.11–0.14], *P*=0.060), Bifrontal index (hypoperfused vs. contralateral: 0.32 [IQR 0.30–0.34] vs. 0.31 [IQR 0.31–0.34], *P*=0.707), Evans index (hypoperfused vs. contralateral: 0.26 [IQR 0.25–0.27] vs. 0.26 [IQR 0.25–0.28], *P*=0.384), Cella index (hypoperfused vs. contralateral: 0.07 [IQR 0.05–0.08] vs. 0.07 [IQR 0.07–0.08], *P*=0.051), Celda media index (hypoperfused vs. contralateral: 5.98 [IQR 5.11–6.68] vs. 5.70 [IQR 4.81–6.21], *P*=0.285), and Ventricular index (hypoperfused vs. contralateral: 0.39 [IQR 0.35–0.45] vs. 0.42 [IQR 0.36–0.51], *P*=0.216) (Fig. 2).

Discussion

Vascular risk factors were considered to increase the risk of AD and cognitive functions, which may be caused by their effects on Aβ metabolism and neurodegeneration in the brain. A recent large prospective cohort study further

206 focused on the relationship between VRFs and AD and found that midlife but not
207 late-life VRFs were significantly associated with elevated amyloid deposition in
208 cognitively normal participants (23). This effect is probably due to insufficient
209 cerebral blood supply, which may impair the function of the neurovascular unit, cause
210 the cerebral hypoperfusion and imbalance between the production and clearance of
211 Aβ, and finally lead to the deterioration of AD pathological changes and cognitive
212 dysfunction(7, 10). Some studies found that there there is cerebral hypoperfusion in
213 the temporal and parietal lobes in AD patients (4).
214 However, whether hypoperfusion can directly lead to the AD-related pathological
215 changes remains uncertain. Previous animal studies have found that cerebral
216 hypoperfusion triggered Aβ deposition in vessel walls parenchyma in the brain. It was
217 found that in a mild chronic cerebral hypoperfusion animal model using C57BL/6J
218 mice subjected to the right common carotid artery permanent ligation, the cerebral
219 hypoperfusion triggered both early vascular deposition of peripherally applied human
220 Aβ1-42 peptides and small stable Aβ deposits in the hypoperfused brain parenchyma
221 6 weeks later *(12).* On the contrary, hypoperfusion was shown to have little or no
222 effect on an altered brain Aβ burden in human studies (13-15), which was consistent
223 with the results of our study. As to the acute hypoperfusion, several studies found that
224 acute stroke was not associated with sustained or increased Aβ deposition (24, 25).
225 Therefore, it is probable that both chronic and acute hypoperfusion does not generate
226 a direct impact on cerebral Aβ deposition.

Some studies found hypoperfusion is associated with progress from MCI to dementia and subsequent cognitive decline in humans (26, 27). However, it remains uncertain whether cerebral hypoperfusion aggravates Aβ deposition and neurodegeneration in AD. In AD transgenic mice, ligation of carotid arteries increased Aβ deposition and neuron loss in the brain (11, 28). But in our study, chronic cerebral hypoperfusion is not associated with increased Aβ deposition and aggravated brain atrophy in a preclinical AD subject who carried APOE ε4 allele and had obvious Aβ deposition in the brain. To our knowledge, there is no direct evidence showing that cerebral hypoperfusion aggravates Aβ deposition in AD patients. This needs to be addressed in the future.

There were some strengths in our study. First, the chronic hypoperfusion of the included subjects all occurred on only one side, and the perfusion of the contralateral side was normal, so the influence of the individual heterogeneity on the results could be eliminated. Second, patients with major stroke were excluded for the potential influence of infarction on Aβ deposition and neurodegeneration. Third, we enrolled relatively older patients with the median age of 64 years old, who were suitable for examing the impact of hypoperfusion on Aβ deposition and neurodegeneration, as AD-related pathological changes are suggested to begin at 15 to 20 years before dementia onset.

The limitation of our study is that the number of participants is relatively small, yet patients with chronic unilateral cerebral hypoperfusion were difficult to enroll in clinical practice. In addition, previous studies suggested that brain microvascular

changes have an impact on the pathology of AD (29), but our study only included the hypoperfusion caused by large blood vessel stenosis, which may not be generalized to hypoperfusion due to small vessel diseases. Third, the duration of hypoperfusion of our participants is unknown. We could not completely exclude the possibility that the duration of hypoperfusion is not long enough to induce cerebral amyloidosis and neurodegeneration in our cohort.

In conclusion, we found that chronic cerebral hypoperfusion due to large vessel lesions is not associated with increased β-amyloid deposition or aggravated brain atrophy, implying that chronic hypoperfusion does not directly induce Aβ deposition and neurodegeneration in the brain.

Ethics approval and consent to participate

This study was approved by the Institutional Review Board of Daping Hospital. Written informed consent was obtained from individual or guardian participants.

Consent for publication

Not applicable

Availability of data and materials

The datasets used and analysed during the study are available from the corresponding author on reasonable request.

Competing interests

There are no potential conflicts of interest.

Funding

This study was supported by National Natural Science Foundation of China (81930028, 81625007, 91749206, 81701043, 81870860, and 31921003).

Authors' contributions

Y.J.W. and F.Z. conceived and designed the project, H.Y.L, Y.C., X.Y., D.W.C., H.Y., Q.Q.S. and F.Z. enrolled the subjects, F.Y.J., Y.T., Q.M.L., F.Y.W. and R.B.J.

conducted the PiB-PET scan, S.N.W. and R.B.J. conducted the CT and MRI scan, D.Y.F. and F.Z. analyzed data, D.Y.F., F.Z. and Y.J.W. wrote the manuscript.

Acknowledgments

The authors are grateful to all participants for their involvement.

References

1. Castellani RJ, Rolston RK, Smith MA. Alzheimer disease. Disease-a-month : DM. 2010;56(9):484-546.

2. Jia J, Wang F, Wei C, Zhou A, Jia X, Li F, et al. The prevalence of dementia in urban and rural areas of China. Alzheimer's & dementia : the journal of the Alzheimer's Association. 2014;10(1):1-9.

3. Selkoe DJ, Hardy J. The amyloid hypothesis of Alzheimer's disease at 25 years. EMBO Mol Med. 2016;8(6):595-608.

4. Chen W, Song X, Beyea S, D'Arcy R, Zhang Y, Rockwood K. Advances in perfusion magnetic resonance imaging in Alzheimer's disease. Alzheimers Dement. 2011;7(2):185-96.

5. Binnewijzend MA, Kuijer JP, Benedictus MR, van der Flier WM, Wink AM, Wattjes MP, et al. Cerebral blood flow measured with 3D pseudocontinuous arterial spin-labeling MR imaging in Alzheimer disease and mild cognitive impairment: a marker for disease severity. Radiology. 2013;267(1):221-30.

6. Chao LL, Pa J, Duarte A, Schuff N, Weiner MW, Kramer JH, et al. Patterns of cerebral hypoperfusion in amnestic and dysexecutive MCI. Alzheimer disease and associated disorders. 2009;23(3):245-52.

7. Iturria-Medina Y, Sotero RC, Toussaint PJ, Mateos-Perez JM, Evans AC, Alzheimer's Disease Neuroimaging I. Early role of vascular dysregulation on late-onset Alzheimer's disease based on multifactorial data-driven analysis. Nat Commun. 2016;7:11934.

8. de la Torre JC. How do heart disease and stroke become risk factors for Alzheimer's disease? Neurological research. 2006;28(6):637-44.

9. de la Torre JC. Impaired cerebromicrovascular perfusion. Summary of evidence in support of its causality in Alzheimer's disease. Annals of the New York Academy of Sciences. 2000;924:136-52.

10. Kume K, Hanyu H, Sato T, Hirao K, Shimizu S, Kanetaka H, et al. Vascular risk factors are associated with faster decline of Alzheimer disease: a longitudinal SPECT study. Journal of neurology. 2011;258(7):1295-303.

11. Pimentel-Coelho PM, Michaud JP, Rivest S. Effects of mild chronic cerebral hypoperfusion and early amyloid pathology on spatial learning and the cellular innate immune response in mice. Neurobiol Aging. 2013;34(3):679-93.

12. ElAli A, Theriault P, Prefontaine P, Rivest S. Mild chronic cerebral hypoperfusion induces neurovascular dysfunction, triggering peripheral beta-amyloid brain entry and aggregation. Acta Neuropathol Commun. 2013;1:75.

13. Hansson O, Palmqvist S, Ljung H, Cronberg T, van Westen D, Smith R. Cerebral hypoperfusion is not associated with an increase in amyloid beta pathology in middle-aged or elderly people. Alzheimers Dement. 2018;14(1):54-61.

14. Yamauchi H, Kagawa S, Takahashi M, Oishi N, Ono M, Higashi T. Misery perfusion and amyloid deposition in atherosclerotic major cerebral artery disease. Neuroimage Clin. 2019;22:101762.

15. Ogasawara K, Fujiwara S, Chida K, Terasaki K, Sasaki M, Kubo Y. Reduction in amyloid beta deposition on (18)F-florbetapir positron emission tomography with correction of cerebral hypoperfusion after endarterectomy for carotid stenosis. Am J Nucl Med Mol Imaging. 2019;9(6):316-20.

16. Folstein MF, Folstein SE, McHugh PR. "Mini-mental state". A practical method for grading the cognitive state of patients for the clinician. Journal of psychiatric research. 1975;12(3):189-98.

17. Lopresti BJ, Klunk WE, Mathis CA, Hoge JA, Ziolko SK, Lu X, et al. Simplified quantification of Pittsburgh Compound B amyloid imaging PET studies: a comparative analysis. Journal of nuclear medicine : official publication, Society of Nuclear Medicine. 2005;46(12):1959-72.

18. Bourgeat P, Villemagne VL, Dore V, Brown B, Macaulay SL, Martins R, et al. Comparison of MR-less PiB SUVR quantification methods. Neurobiol Aging. 2015;36 Suppl 1:S159-66.

19. Palmqvist S, Zetterberg H, Blennow K, Vestberg S, Andreasson U, Brooks DJ, et al. Accuracy of brain amyloid detection in clinical practice using cerebrospinal fluid

346 beta-amyloid 42: a cross-validation study against amyloid positron emission
347 tomography. JAMA Neurol. 2014;71(10):1282-9.
348 20. Meese W, Kluge W, Grumme T, Hopfenmüller W. CT evaluation of the CSF
349 spaces of healthy persons. Neuroradiology. 1980;19(3):131-6.
350 21. Romero-Acevedo L, Gonzalez-Reimers E, Martin-Gonzalez MC, Gonzalez-Diaz
351 A, Quintero-Platt G, Reyes-Suarez P, et al. Handgrip strength and lean mass are
352 independently related to brain atrophy among alcoholics. Clin Nutr.
353 2019;38(3):1439-46.
354 22. Chrzan R, Glen A, Bryll A, Urbanik A. Computed Tomography Assessment of
355 Brain Atrophy in Centenarians. Int J Environ Res Public Health. 2019;16(19).
356 23. Gottesman RF, Schneider AL, Zhou Y, Coresh J, Green E, Gupta N, et al.
357 Association Between Midlife Vascular Risk Factors and Estimated Brain Amyloid
358 Deposition. Jama. 2017;317(14):1443-50.
359 24. Sahathevan R, Linden T, Villemagne VL, Churilov L, Ly JV, Rowe C, et al.
360 Positron Emission Tomographic Imaging in Stroke: Cross-Sectional and Follow-Up
361 Assessment of Amyloid in Ischemic Stroke. Stroke. 2016;47(1):113-9.
362 25. Wollenweber FA, Därr S, Müller C, Duering M, Buerger K, Zietemann V, et al.
363 Prevalence of Amyloid Positron Emission Tomographic Positivity in Poststroke Mild
364 Cognitive Impairment. Stroke. 2016;47(10):2645-8.
365 26. Quaranta D, Gainotti G, Di Giuda D, Vita MG, Cocciolillo F, Lacidogna G, et al.
366 Predicting progression of amnesic MCI: The integration of episodic memory
367 impairment with perfusion SPECT. Psychiatry Res Neuroimaging. 2018;271:43-9.

27. Chao LL, Buckley ST, Kornak J, Schuff N, Madison C, Yaffe K, et al. ASL perfusion MRI predicts cognitive decline and conversion from MCI to dementia. Alzheimer Dis Assoc Disord. 2010;24(1):19-27.

28. Okamoto Y, Yamamoto T, Kalaria RN, Senzaki H, Maki T, Hase Y, et al. Cerebral hypoperfusion accelerates cerebral amyloid angiopathy and promotes cortical microinfarcts. Acta Neuropathol. 2012;123(3):381-94.

29. Østergaard L, Aamand R, Gutiérrez-Jiménez E, Ho YC, Blicher JU, Madsen SM, et al. The capillary dysfunction hypothesis of Alzheimer's disease. Neurobiol Aging. 2013;34(4):1018-31.

FIGURE LEGENDS

Figure 1. Hypoperfusion and β-amyloid burden. SUVRs of ^{11}C-PiB of the hypoperfused cortex (Ctx_{Hypo}) and normally-perfused control cortex (Ctx_{Ctrl}) in VOI (A) and ROI (B). The cortex/white matter ratio of the hypoperfused region (Ctx_H/Wm_H) and normally-perfused control cortex (Ctx_C/Wm_C) in VOI (C) and ROI (D). SUVR, standardized uptake value ratio; Ctx, cerebral cortex; Wm, cerebral white matter. Hypo, hypoperfused hemisphere; Ctrl, contralateral hemisphere. Error bars, interquartile range.

Figure 2. Hypoperfusion and brain atrophy. Brain atrophy indices of the bilateral hemisphere (A-F). CT indices used in this study (G). Bicaudate index = minimum width of lateral ventricles/skull width at the same level = B/E. Bifrontal index = maximum width of frontal horns/skull width at the same level = A/D. Evans index = maximum width of frontal horns/skull width at the level of the third ventricle = A/F. Cella index = width of the third ventricle/skull width at the same level = C/F. Celda media index = maximum width of the skull/width of lateral ventricles = G/H. Ventricular index = minimum width of lateral ventricles/maximum width of frontal horns = B/A. Hypo, hypoperfused hemisphere; Ctrl, contralateral hemisphere. Error bars, interquartile range.

Figure 3. Multimodal imaging. Images of cases: 1, 3, 4, 5, 8, 9 (A-F) are presented by CT, cerebral blood flow (CBF), mean transit time (MTT), ^{11}C-PiB-PET SUVRs in VOI, and ^{11}C-PiB-PET SUVRs in ROI. Circles and irregular enclosed regions indicate the location of analysis, where red represents the hypoperfusion region and

white represents the normally-perfused control region. Arrows indicate an area with ^{11}C-PiB retention related to cerebral infarction. CT, Computed Tomography; SUVRs, standardized uptake value ratios.

Figures

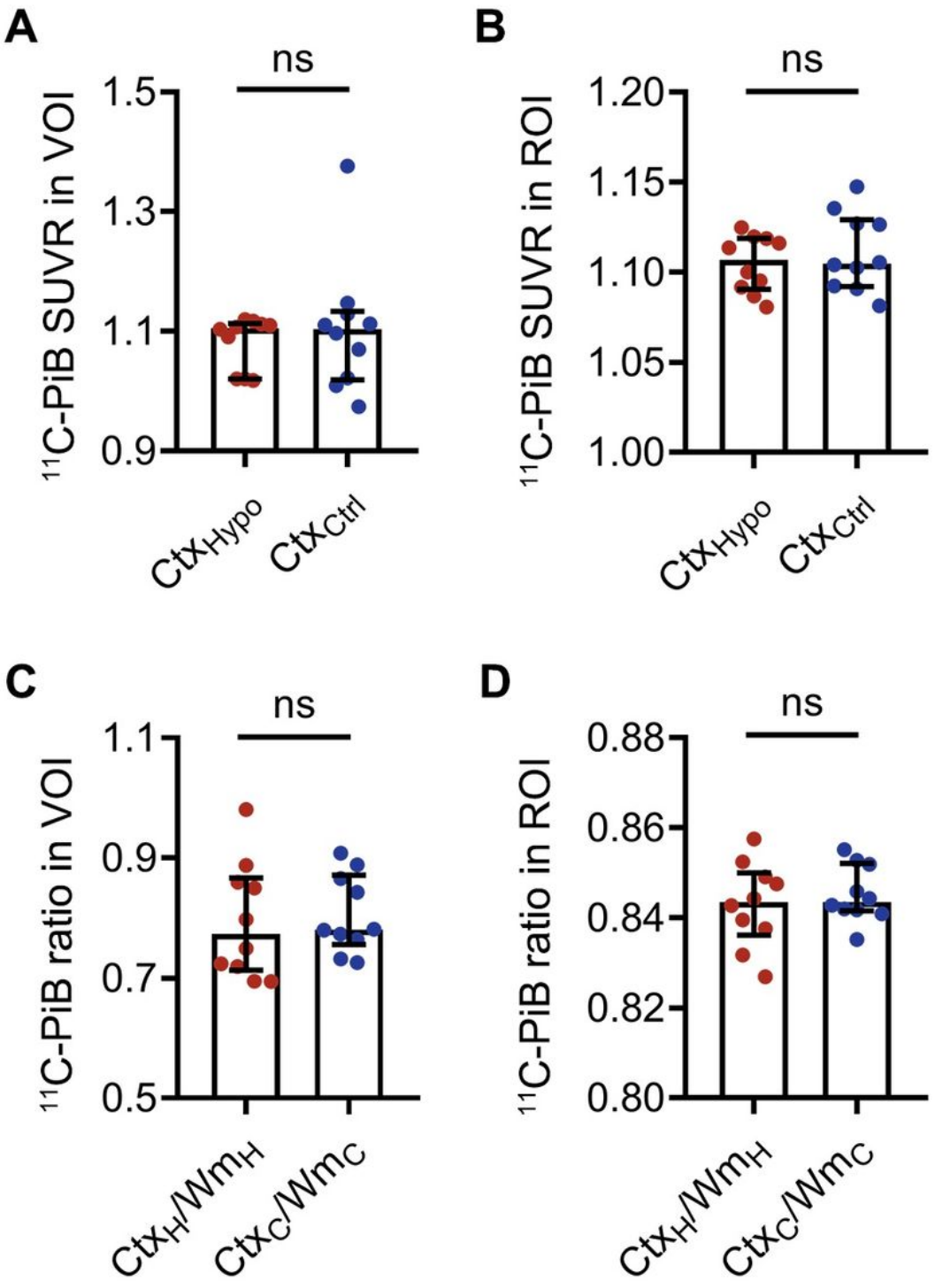

Figure 1

Hypoperfusion and β-amyloid burden. SUVRs of 11C-PiB of the hypoperfused cortex (CtxHypo) and normally-perfused control cortex (CtxCtrl) in VOI (A) and ROI (B). The cortex/white matter ratio of the hypoperfused region (CtxH/WmH) and normally-perfused control cortex (CtxC/WmC) in VOI (C) and ROI

(D). SUVR, standardized uptake value ratio; Ctx, cerebral cortex; Wm, cerebral white matter. Hypo, hypoperfused hemisphere; Ctrl, contralateral hemisphere. Error bars, interquartile range.

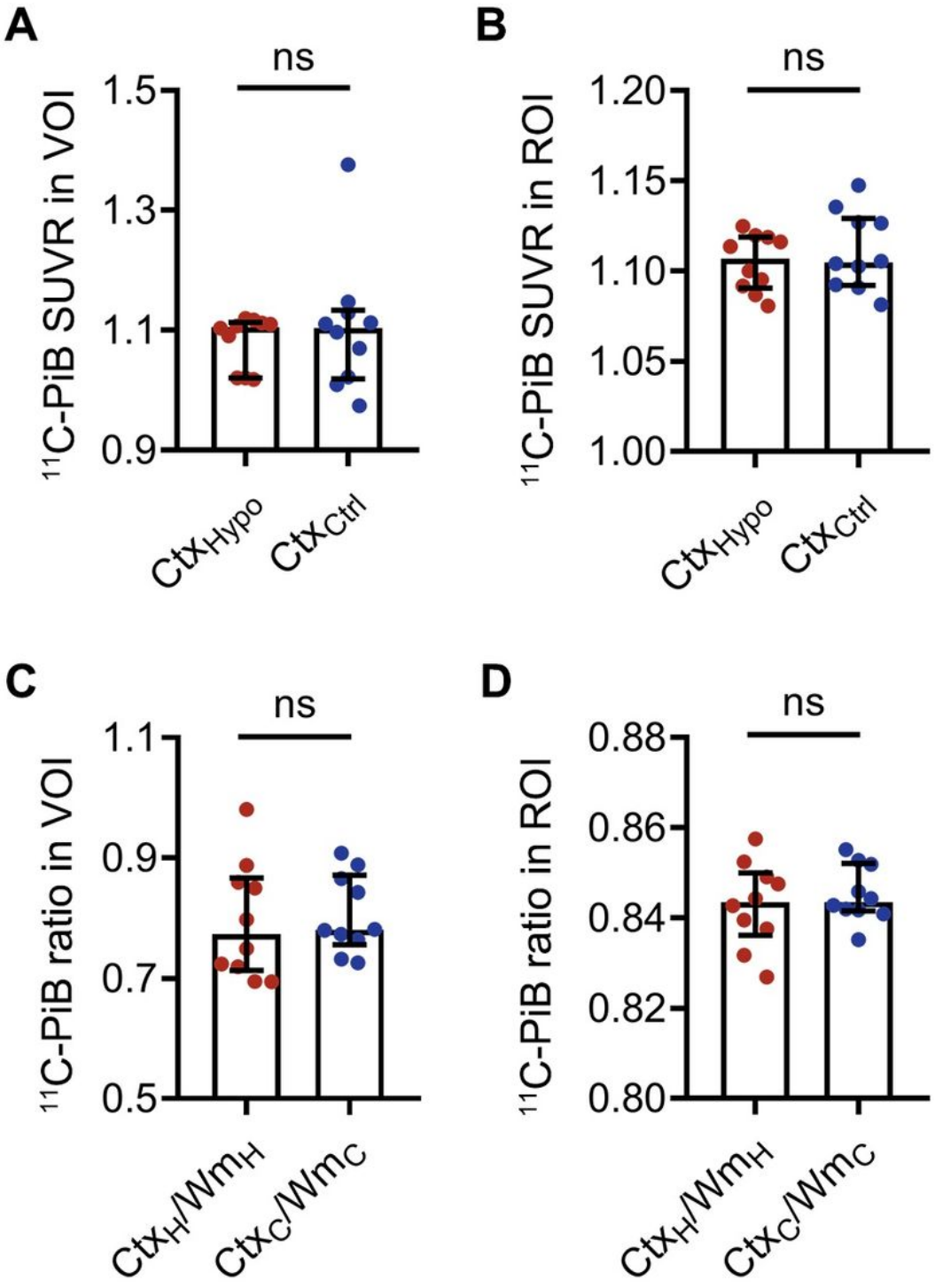

Figure 1

Hypoperfusion and β-amyloid burden. SUVRs of 11C-PiB of the hypoperfused cortex (CtxHypo) and normally-perfused control cortex (CtxCtrl) in VOI (A) and ROI (B). The cortex/white matter ratio of the hypoperfused region (CtxH/WmH) and normally-perfused control cortex (CtxC/WmC) in VOI (C) and ROI

(D). SUVR, standardized uptake value ratio; Ctx, cerebral cortex; Wm, cerebral white matter. Hypo, hypoperfused hemisphere; Ctrl, contralateral hemisphere. Error bars, interquartile range.

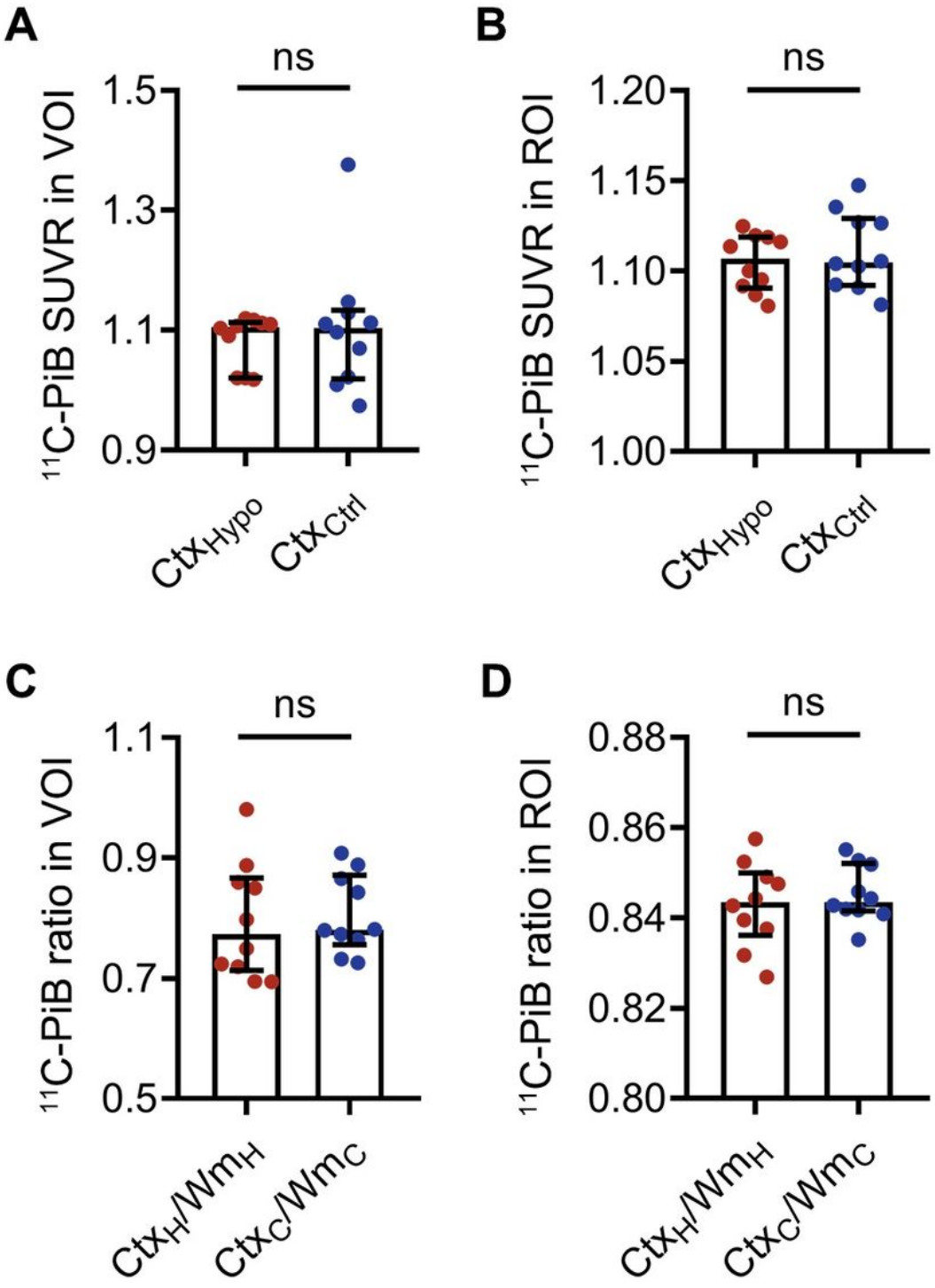

Figure 1

Hypoperfusion and β-amyloid burden. SUVRs of 11C-PiB of the hypoperfused cortex (CtxHypo) and normally-perfused control cortex (CtxCtrl) in VOI (A) and ROI (B). The cortex/white matter ratio of the hypoperfused region (CtxH/WmH) and normally-perfused control cortex (CtxC/WmC) in VOI (C) and ROI

(D). SUVR, standardized uptake value ratio; Ctx, cerebral cortex; Wm, cerebral white matter. Hypo, hypoperfused hemisphere; Ctrl, contralateral hemisphere. Error bars, interquartile range.

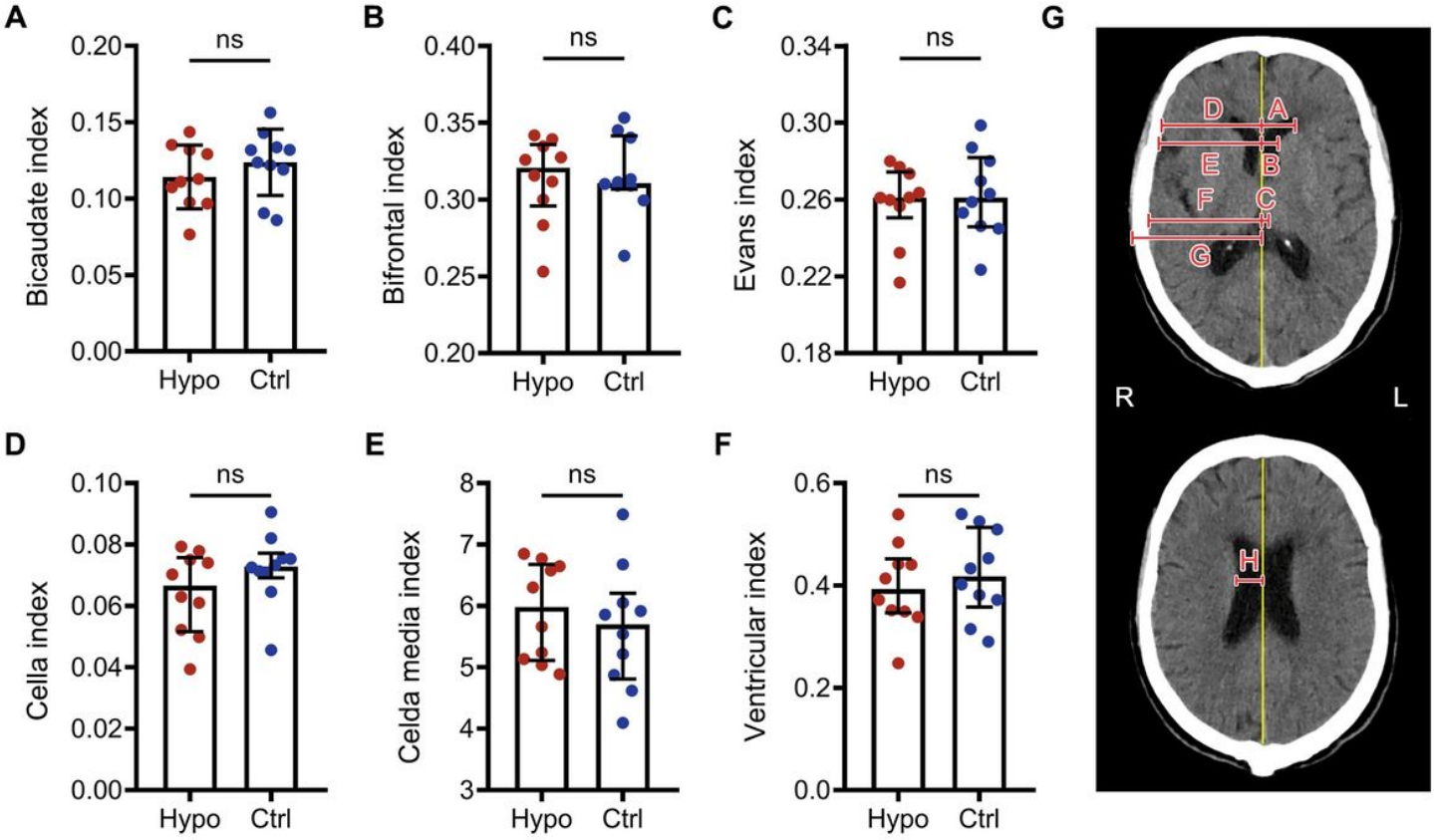

Figure 2

Hypoperfusion and brain atrophy. Brain atrophy indices of the bilateral hemisphere (A-F). CT indices used in this study (G). Bicaudate index = minimum width of lateral ventricles/skull width at the same level = B/E. Bifrontal index = maximum width of frontal horns/skull width at the same level = A/D. Evans index = maximum width of frontal horns/skull width at the level of the third ventricle = A/F. Cella index = width of the third ventricle/skull width at the same level = C/F. Celda media index = maximum width of the skull/width of lateral ventricles = G/H. Ventricular index = minimum width of lateral ventricles/maximum width of frontal horns = B/A. Hypo, hypoperfused hemisphere; Ctrl, contralateral hemisphere. Error bars, interquartile range.

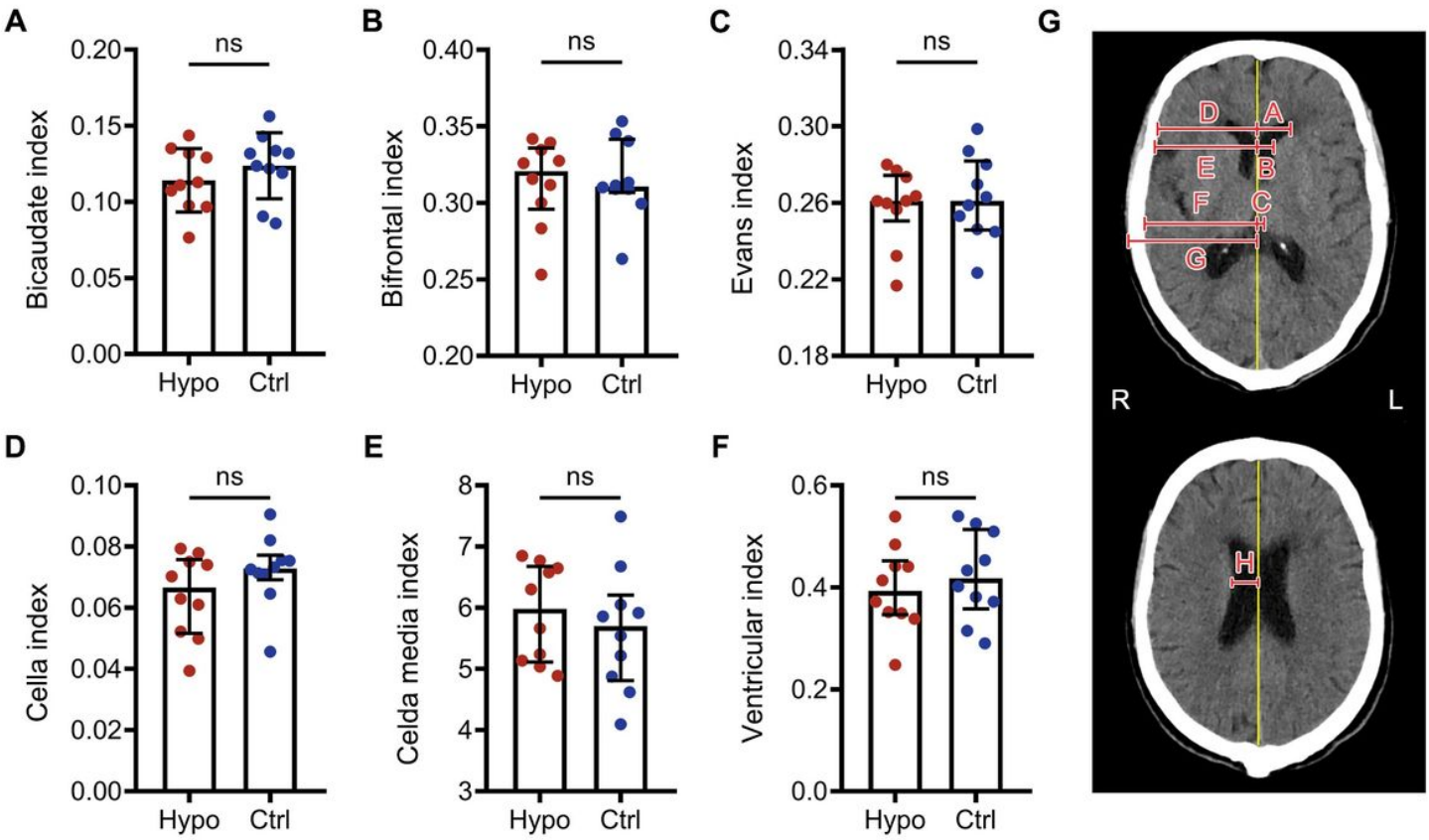

Figure 2

Hypoperfusion and brain atrophy. Brain atrophy indices of the bilateral hemisphere (A-F). CT indices used in this study (G). Bicaudate index = minimum width of lateral ventricles/skull width at the same level = B/E. Bifrontal index = maximum width of frontal horns/skull width at the same level = A/D. Evans index = maximum width of frontal horns/skull width at the level of the third ventricle = A/F. Cella index = width of the third ventricle/skull width at the same level = C/F. Celda media index = maximum width of the skull/width of lateral ventricles = G/H. Ventricular index = minimum width of lateral ventricles/maximum width of frontal horns = B/A. Hypo, hypoperfused hemisphere; Ctrl, contralateral hemisphere. Error bars, interquartile range.

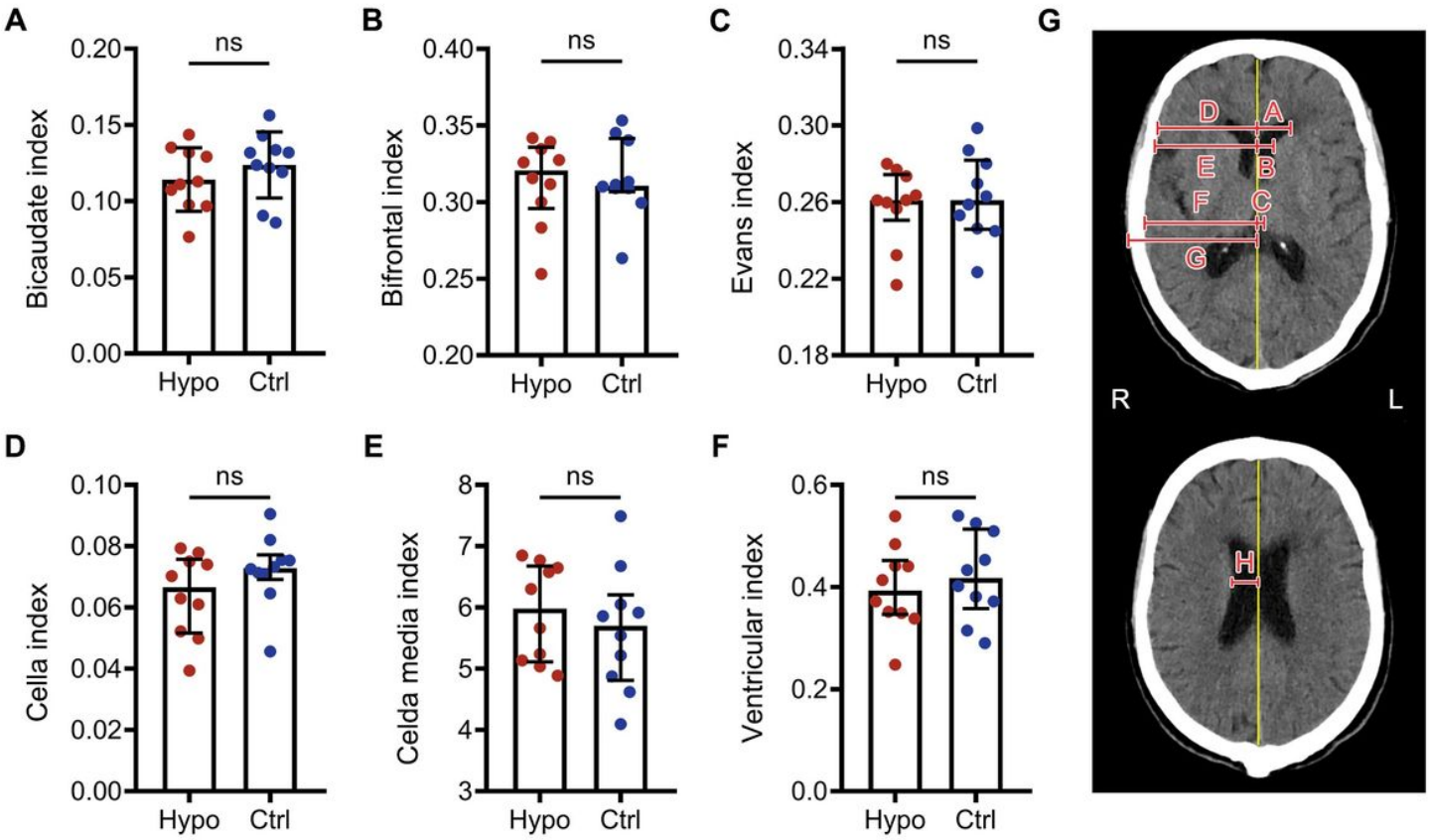

Figure 2

Hypoperfusion and brain atrophy. Brain atrophy indices of the bilateral hemisphere (A-F). CT indices used in this study (G). Bicaudate index = minimum width of lateral ventricles/skull width at the same level = B/E. Bifrontal index = maximum width of frontal horns/skull width at the same level = A/D. Evans index = maximum width of frontal horns/skull width at the level of the third ventricle = A/F. Cella index = width of the third ventricle/skull width at the same level = C/F. Celda media index = maximum width of the skull/width of lateral ventricles = G/H. Ventricular index = minimum width of lateral ventricles/maximum width of frontal horns = B/A. Hypo, hypoperfused hemisphere; Ctrl, contralateral hemisphere. Error bars, interquartile range.

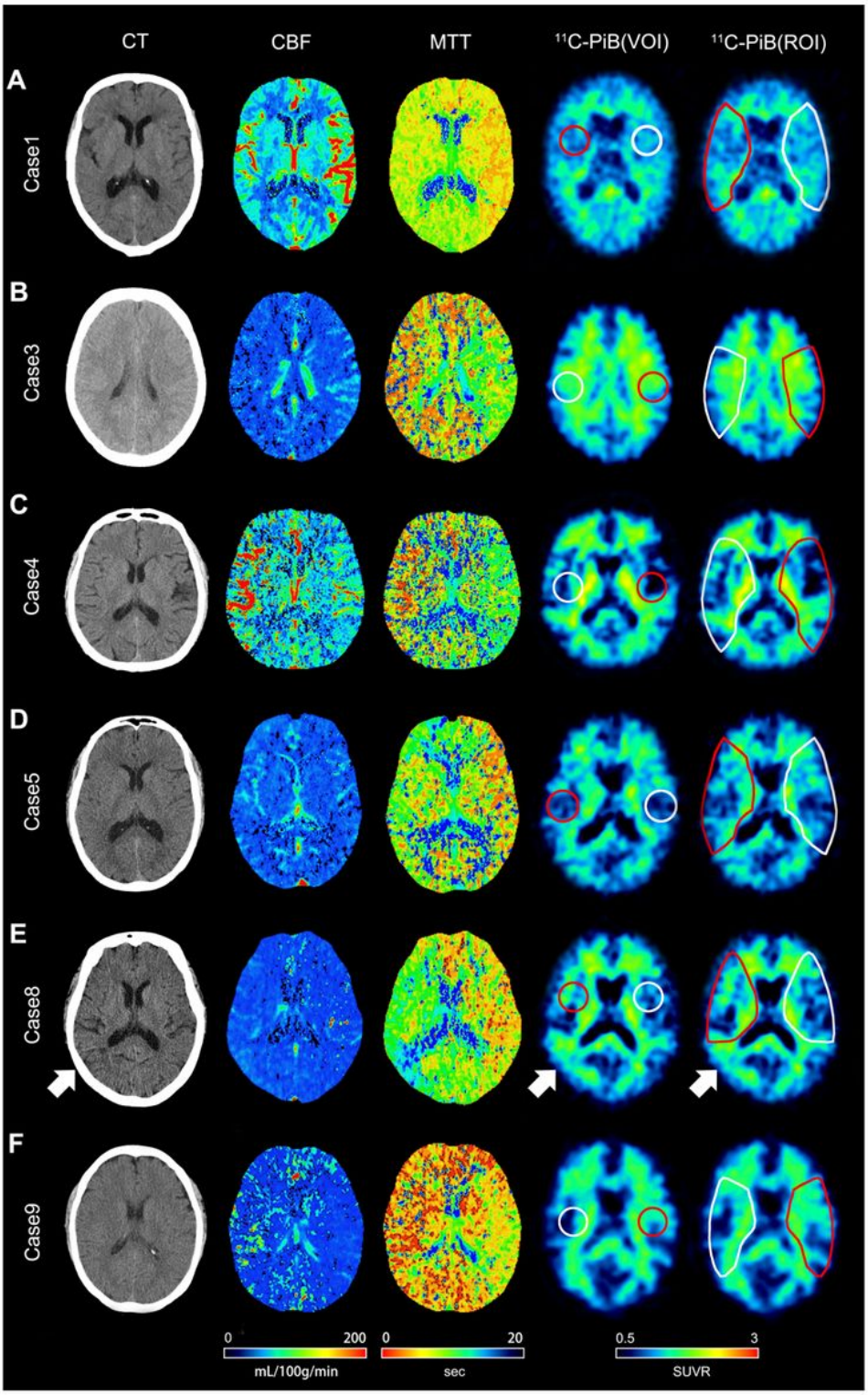

Figure 3

Multimodal imaging. Images of cases: 1, 3, 4, 5, 8, 9 (A-F) are presented by CT, cerebral blood flow (CBF), mean transit time (MTT), 11C-PiB-PET SUVRs in VOI, and 11C-PiB-PET SUVRs in ROI. Circles and irregular enclosed regions indicate the location of analysis, where red represents the hypoperfusion region and white represents the normally-perfused control region. Arrows indicate an area with 11C-PiB retention related to cerebral infarction. CT, Computed Tomography; SUVRs, standardized uptake value ratios.

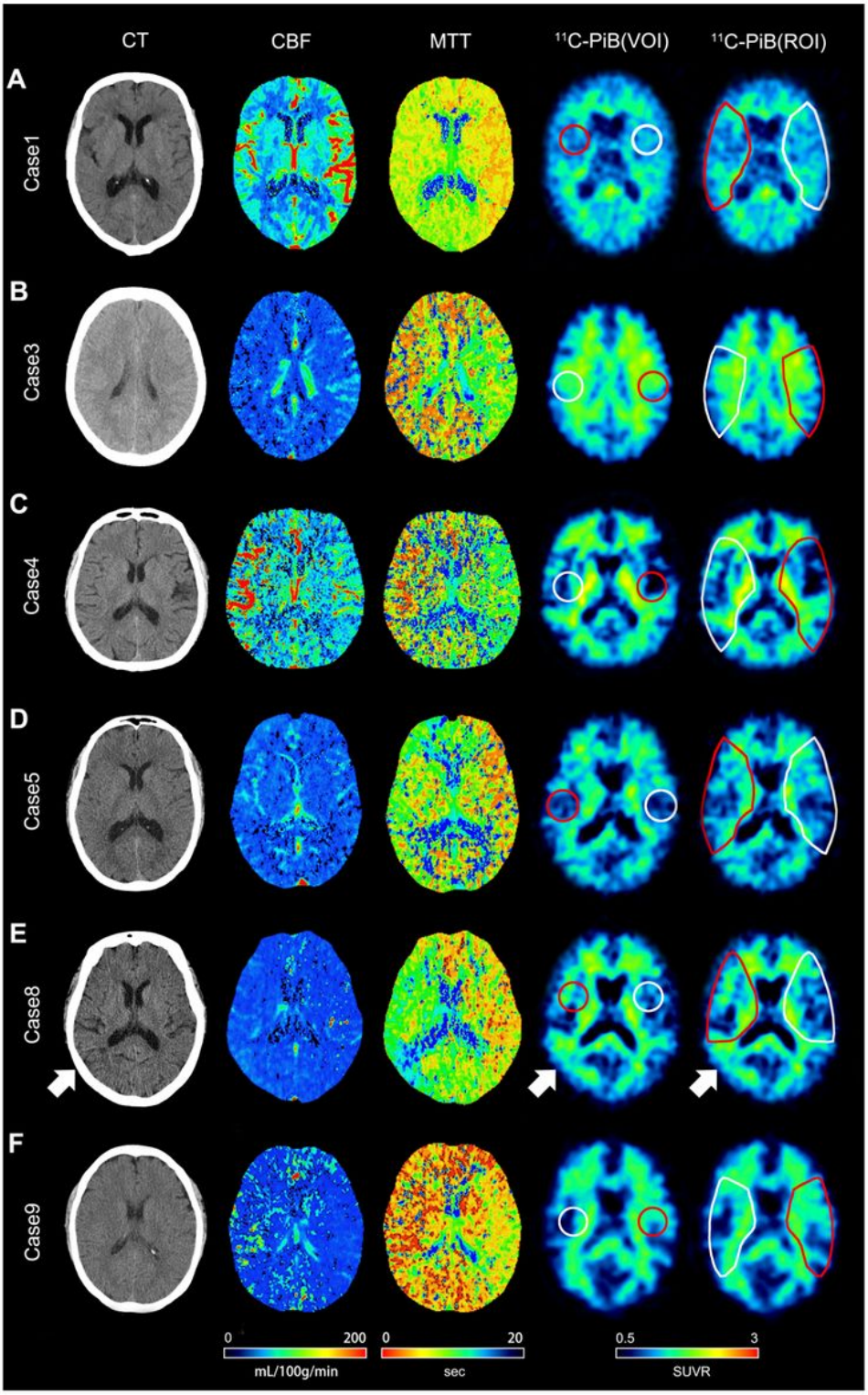

Figure 3

Multimodal imaging. Images of cases: 1, 3, 4, 5, 8, 9 (A-F) are presented by CT, cerebral blood flow (CBF), mean transit time (MTT), 11C-PiB-PET SUVRs in VOI, and 11C-PiB-PET SUVRs in ROI. Circles and irregular enclosed regions indicate the location of analysis, where red represents the hypoperfusion region and white represents the normally-perfused control region. Arrows indicate an area with 11C-PiB retention related to cerebral infarction. CT, Computed Tomography; SUVRs, standardized uptake value ratios.

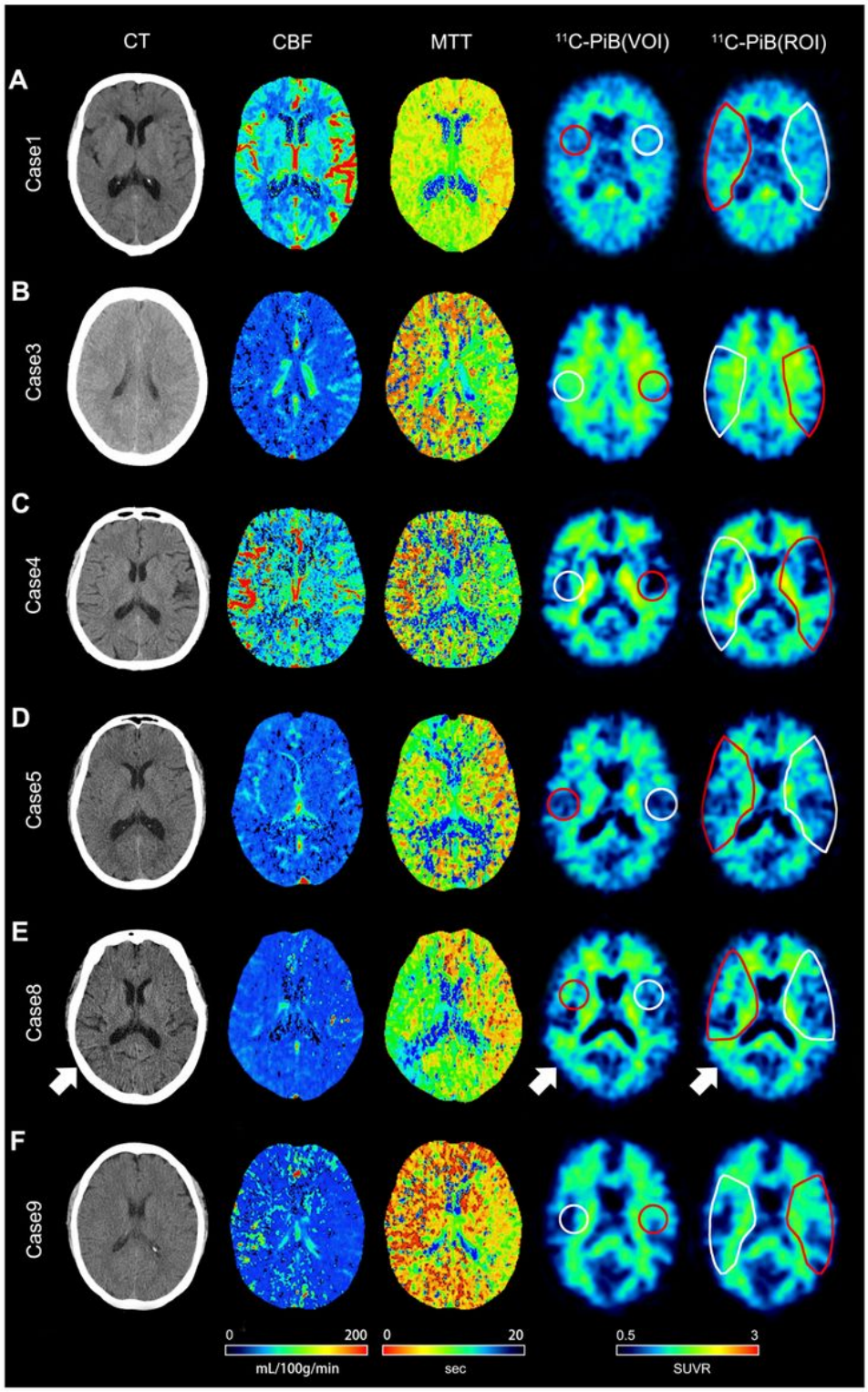

Figure 3

Multimodal imaging. Images of cases: 1, 3, 4, 5, 8, 9 (A-F) are presented by CT, cerebral blood flow (CBF), mean transit time (MTT), 11C-PiB-PET SUVRs in VOI, and 11C-PiB-PET SUVRs in ROI. Circles and irregular enclosed regions indicate the location of analysis, where red represents the hypoperfusion region and white represents the normally-perfused control region. Arrows indicate an area with 11C-PiB retention related to cerebral infarction. CT, Computed Tomography; SUVRs, standardized uptake value ratios.

Supplementary Files

This is a list of supplementary files associated with this preprint. Click to download.

- Table1Characteristicsofthestudysubjects.docx
- Table1Characteristicsofthestudysubjects.docx
- Table1Characteristicsofthestudysubjects.docx